Single-Particle Analysis of Aerosols at Cheju Island, Korea, Using Low- Z Electron Probe X-ray Microanalysis: A Direct Proof of Nitrate Formation from Sea Salts

ARTICLE *in* ENVIRONMENTAL SCIENCE AND TECHNOLOGY · DECEMBER 2001

Impact Factor: 5.33 · DOI: 10.1021/es0155231 · Source: PubMed

Environ. Sci. Technol. **2001**, *35,* 4487−4494

Single-Particle Analysis of Aerosols at Cheju Island, Korea, Using Low-*Z* Electron Probe X-ray Microanalysis: A Direct Proof of Nitrate Formation from Sea Salts

CHUL-UN RO,*,†,‡ KEUN-YOUNG OH,† HYEKYEONG KIM,‡ YONG PYO KIM,§ CHONG BUM LEE,|| KI-HYUN KIM,⊥ CHANG HEE KANG,# JÁNOS OSÁN,▽ JOHAN DE HOOG,○ ANNA WOROBIEC,○ AND RENÉ VAN GRIEKEN○

Department of Chemistry, Hallym University, Chun Cheon, Kang Won Do, 200-702 Korea, Institute of Environment & Life Science, Hallym Academy of Sciences, Hallym University, Chun Cheon, Kang Won Do, 200-702 Korea, Department of Environmental Science and Engineering, Ewha Womans University, Seoul, 120-750 Korea, Department of Environmental Science, Kangwon National University, Chun Cheon, Kang Won Do, 200-701 Korea, Department of Earth Sciences, Sejong University, Seoul, 143-747 Korea, Department of Chemistry, Cheju National University, Cheju, 690-756 Korea, KFKI Atomic Energy Research Institute, P.O. Box 49, H-1525 Budapest, Hungary, and Department of Chemistry, University of Antwerp, Universiteitsplein 1, B-2610 Antwerp, Belgium

A recently developed electron probe X-ray microanalysis (EPMA), called low-*Z* EPMA, employing an ultrathin window energy-dispersive X-ray detector, was applied to characterize aerosol particles collected at two sampling sites, namely, Kosan and 1100 Hill of Cheju Island, Korea, on a summer day in 1999. Since low-*Z* EPMA can provide quantitative information on the chemical composition of aerosol particles, the collected aerosol particles were classified and analyzed based on their chemical species. Many different particle types were identified, such as marine-originated, carbonaceous, soil-derived, and anthropogenic particles. Marine-originated particles, such as $NaNO_3$- and Na_2SO_4-containing particles, are very frequently encountered in the two samples. In this study, it was directly proven that the observed nitrate particles were from sea salts. In addition, two types of nitrate particles from sea salts were observed, with and without Mg. The sodium nitrate particles without Mg were believed to be collected as crystalline form, either with the sodium nitrate particles being fractionally recrystallized within evaporating seawater drops or with recrystallized sodium chloride particles having reacted with gaseous nitrogen species in the air to form the crystalline sodium nitrate particles. The other seemed to be collected as seawater drops, where the atmospheric reaction had occurred in the droplets, and thus sodium as well as magnesium nitrates were observed. Carbonaceous particles are the most abundant in the samples at both sites. From this study, it was found that about three-quarters of the carbonaceous particles in the samples were biogenic, which partially explains a previously reported observation of a large concentration of organic carbon particles as compared to elemental carbon. Various soil-derived particles were also observed. In addition to aluminosilicate- and iron oxide-containing particles, which are ubiquitous components in soil-derived particles, $CaCO_3$-, Al_2O_3- and Cr-containing particles were also frequently encountered.

Introduction

Characterization of airborne particles deepens our understanding about the source, reactivity, transport, and removal of atmospheric chemical species. Since atmospheric particles are chemically and morphologically heterogeneous and the average composition and the average aerodynamic diameter do not describe well the population of the particles, microanalytical methods have proven to be useful for studying atmospheric particles. Electron probe X-ray microanalysis (EPMA) is capable of simultaneously detecting the chemical composition and the morphology of a microscopic volume such as a single atmospheric particle (*1*). A recently developed EPMA technique, called low-*Z* EPMA, allows the determination of the concentration of low-*Z* elements such as carbon, nitrogen, and oxygen, as well as higher-*Z* elements, which are observed using conventional energy-dispersive EPMA (ED-EPMA) (*2*−*4*). By the application of the low-*Z* EPMA technique, which employs an ultrathin window energy-dispersive X-ray (EDX) detector, chemical compositions, including the low-*Z* components, of individual particles can be quantitatively elucidated. The determination of low-*Z* elements in individual environmental particles allows the improvement of the applicability of single-particle analysis; many environmentally important atmospheric particles (e.g., sulfates, nitrates, ammonium, and carbonaceous particles) contain low-*Z* elements. Furthermore, the diversity of atmospheric particles in chemical composition can be investigated in detail using the low-*Z* EPMA technique.

Application of wavelength-dispersive X-ray (WDX) detection is another possibility for quantitative low-*Z* element analysis. Recently, it was shown that semiquantitative WDX analysis, down to oxygen, is feasible even for irregularly shaped particles down to 0.8 μm in equivalent diameter (*5*). The WDX approach has some advantages over EDX in terms of its better detection limit for low-*Z* elements, due to its better peak-to-background ratio, and its superior energy resolution, resulting in a lower probability of the overlapping between low-*Z* element K- and L-lines of transition metals. However, most critically, the much higher current needed for the measurements in WDX limits its potential just to the particles that are most stable under electron bombardment.

There have been approaches to specify environmentally important chemical species in individual particles, e.g., nitrate and sulfate, using EPMA (*6*−*9*). These techniques employ chemical reactions on individual particles of interest; for example, barium chloride and Nitron are used as reaction

* Corresponding author telephone: +82 33 240 1428; fax: +82 33 256 3421; e-mail: curo@hallym.ac.kr.
† Department of Chemistry, Hallym University.
‡ Hallym Academy of Sciences, Hallym University.
§ Ewha Womans University.
|| Kangwon National University.
⊥ Sejong University.
Cheju National University.
▽ KFKI Atomic Energy Research Institute.
○ University of Antwerp.

10.1021/es0155231 CCC: $20.00
Published on Web 10/18/2001

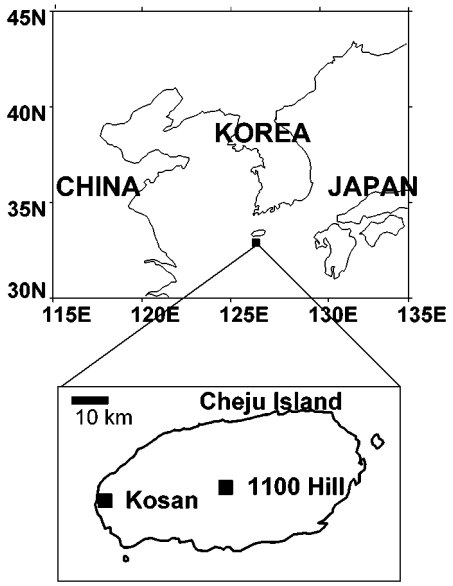

FIGURE 1. Location of the measurement sites and surrounding region.

agents for sulfate and nitrate species, respectively. The particles with nitrate or sulfate react with those agents to produce characteristic morphologies if reaction occurs so that those particles can be identified using either scanning or transmission electron microscopy. These techniques have proven to be useful to study the atmospheric chemistry of nitrate or sulfate species in the reaction with other airborne particles, such as sea salt, mineral, and carbonaceous particles. However, these techniques only allow the analysis of nitrate and sulfate species; furthermore, this analysis is purely qualitative since only the presence or the absence of those chemical species can be determined.

Another single-particle analysis technique allows the identification of chemical species of individual particles qualitatively using laser microprobe mass spectrometry, the so-called ATOFMS (*10*−*12*). This technique can analyze the aerodynamic sizes and chemical compositions of individual particles in real time, and even the instrument can be portable (*12*) so that it can be used in the field. By application of the ATOFMS technique, the complex nature of airborne particles has been directly revealed (*13*, *14*), and it was demonstrated that the technique can clearly elucidate the atmospheric chemistry between sea-salt particles and gas-phase nitric acid as it occurs in the atmosphere (*15*). However, due to its poor reproducibility, the technique can now only provide qualitative determination of chemical species in individual particles.

The low-*Z* EPMA was applied to characterize aerosols collected at Cheju Island, Korea. Cheju Island is an ideal place to study continental and marine influences on aerosols because it is surrounded by the Korean peninsula, mainland China, Japan, and the China Sea (see Figure 1), and it is also one of the cleanest areas in Korea. Several extensive works on the aerosol composition on the island have already been carried out, such as studies on summertime characteristics of the aerosol including carbonaceous species (*16*), seasonal variation of the overall aerosol composition (*17*−*21*), and seasonal variation of particulate nitrate (*22*). Also, two modeling studies were performed to understand the seasonal behavior of the aerosol composition (*23*) and the aging processes of sea-salt and mineral aerosols (*24*) on this island. These studies emphasize the importance of this island as a sampling site for the study of long-range transport of aerosols in northeastern Asia where emission of air pollutants is considerably large (*25*). However, no single-particle analysis has been applied to aerosols at Cheju Island until now, which may provide detailed and new information on the chemical composition of the aerosols. We performed single-particle analysis for samples collected on a summer day in 1999. In this work, aerosol samples collected at Kosan and 1100 Hill of Cheju Island were characterized by using the low-*Z* EPMA. Detailed information on chemical composition and size distribution of the particle samples were provided by this single-particle analysis. From this study, we report some new findings on chemical compositions of the aerosol particles in Cheju Island and also a direct proof of nitrate formation from sea salts. However, this study presents more questions than answers on the characteristics of aerosols at Cheju Island. Currently, an international research project, called Aerosol Characterization Experiment—Asia (ACE-Asia), is being carried out until 2004 (homepage: http://saga.pmel.noaa.gov/aceasia) to understand the characteristics of aerosols in northeastern Asia in more detail. Kosan is one of the focal sampling sites for this project. By continuing the single-particle analysis using the low-*Z* EPMA at this sampling site, we hope to clearly address the new questions raised by this work.

Experimental Section

Samples. Samplings were done at two different sampling sites on Cheju Island, namely, Kosan and 1100 Hill (see Figure 1). The Kosan sampling site (33°17′ N, 126°10′ E; altitude, 60 m) is just 10 m away from the coast, and the 1100 Hill site (33°21′ N, 126°27′ E; altitude, 1100 m) is located in the middle of a forest on the slope of Halla Mountain with an elevation of 1950 m. The distance between the two sites is ca. 30 km. Each set of aerosol samples was collected at the two sites on June 19, 1999. Particles were sampled on Ag foil using a seven-stage May cascade impactor (*26*). Sampling was from 9:40 to 11:50 am at Kosan and from 2:20 to 3:30 pm at 1100 Hill. The sampling duration varied between 2 (for stage 6) and 128 (for stage 1) min at Kosan to obtain a good loading of particles at the impaction slots. At 1100 Hill, it was approximately half of that at Kosan, implying higher aerosol concentrations at 1100 Hill during the sampling time. The May impactor has, at a 20 L/min sampling flow, aerodynamic cutoffs of 16, 8, 4, 2, 1, 0.5, and 0.25 μm for stages 1−7, respectively. The seventh stage was not analyzed because the very small size of particles collected on the stage was not suitable for EPMA measurements. Some 300 particles for each stage sample, except stage 6 sample collected at Kosan, were analyzed; in total, there were 2888 particles. The May impactor has an impacting slit at each stage, and thus the aerosols collected on the Ag foil substrate show a slit pattern. A distinct slit line on stage 6 of the sample collected at Kosan was seen just after aerosol collection, and yet it was not possible to find the aerosols under electron microscopy. This was a unique occasion in our measurements, and the explanation for this is that mostly moisture aerosols might be collected at stage 6, of which the aerodynamic cutoff diameter is 0.5 μm, and then they evaporated during storage or under vacuum in the EPMA instrument. On the day before the sampling time, it had rained all day, and some of fine particles might be washed out before our sampling. The collected samples were put in plastic carriers, sealed, and stored in a desiccator.

EPMA Measurements and Data Analysis. The measurements were carried out on a JEOL 733 electron probe microanalyzer equipped with an Oxford Link SATW ultrathin window EDX detector. The resolution of the detector is 133 eV for Mn Kα X-rays. The spectra were recorded by a Canberra S100 multichannel analyzer under control of homemade software. To achieve optimal experimental conditions such as low level of the background in the spectra and high sensitivity for light element analysis, a 10-kV accelerating voltage was chosen. The beam current was 1.0 nA for all the

measurements. To obtain statistically enough counts in the X-ray spectra and to minimize the beam damage effect on the sensitive particles, a typical measuring time of 10 s was used. The cold stage of the electron microprobe allowed the analysis of particulate samples at liquid nitrogen temperature (around −193 °C), which enabled us to minimize contamination and reduce beam damage to the samples as well. A more detailed discussion on the measurement conditions is given elsewhere (*2*). The size and shape of each individual particle was measured from backscattered electron images, and its size was estimated as that of an equivalent spherical particle using a homemade computer program while the X-ray spectrum for each particle was automatically acquired under the control of a computer.

The net X-ray intensities for the elements were obtained by nonlinear least-squares fitting of the collected spectra using the AXIL program (*27*), and the elemental concentrations for individual particles were obtained from their X-ray intensities by application of a Monte Carlo calculation with reverse successive approximations. The Monte Carlo calculation is based on a modified version of the single scattering CASINO Monte Carlo program (*28, 29*), which was designed for low-energy beam interaction generating X-ray and electron signals. The modified version of the CASINO program allows the simulation of electron trajectories in spherical, hemispherical, and hexahedral particles located on a flat substrate (*2*). The simulation procedure determines also the characteristic and continuous X-ray flux emitted from the substrate material and the influence of the substrate material on the energy distribution of the exciting electrons. The quantification procedure uses an iterative approach; the iterative calculation is finished when measured X-ray intensities for all chemical elements in a particle are well matched to intensities simulated by the Monte Carlo calculation. In the beginning of the iterative Monte Carlo calculation, the differences between measured and calculated intensities are considerable so that a successive approximation approach is employed to find the best match, with adjusting input values, e.g., chemical compositions, for the following iteration. When convergency is achieved, the chemical compositions used for the calculation is the obtained chemical composition of the particle. Generally a few iterations are enough to find convergency. The quantification procedure provides good accuracy within around 12% relative deviations between the calculated and the nominal elemental concentrations when the method is applied to various types of standard particles such as NaCl, SiO_2, $CaSO_4 \cdot 2H_2O$, $(NH_4)_2SO_4$, and NH_4NO_3 (*30*). More details on the quantification procedure can be found elsewhere (*4*).

Results and Discussion

Classification of Individual Particles according to Their Chemical Species. The determination of chemical species in individual particles was done in a way to fully utilize the information contained in their X-ray data. The chemical composition of each particle is never exactly the same as that of others; it is rather rare to see particles composed of only one pure chemical species, and also particles with two or more chemical species have different compositions. Since the low-*Z* EPMA can provide quantitative information on chemical composition, we tried to classify particles based, as much as possible, on their chemical species. The analytical procedure for determining chemical species is described in more detail elsewhere (*31*). Here, we briefly summarize how the particle types are classified; first, particles are regarded to be composed of just one chemical species when the chemical species constitutes at least 90% in atomic fraction. Second, it was tried to specify chemical species even for particles internally mixed with two or more chemical species. Third, it is known that ED-EPMA has high detection limits of 0.1−1.0% in weight, mainly due to its high background level. Since the low-*Z* EPMA is used for the analysis of a microscopic volume (picogram range in mass for a single particle of micrometer size), the elements at trace levels could not be reliably investigated. Thus, we do not include elements with less than 1.0% of atomic concentration in the procedure of chemical speciation.

TABLE 1. Particle Types and Numbers of Particles Found in Kosan Sample[a]

	no. of particles					
particle type	stage 1	stage 2	stage 3	stage 4	stage 5	sum
Al_2O_3	6			1		7
AlSi[b]	11	5	15	7	28	66
AlSi/carb[c]	2	3				5
biogenic	37	62	74	61	3	216
carbon-rich	3	2	9	5		19
organic	2	2	16	13	11	44
$CaCO_3$	8	5	6	6	1	26
$CaSO_4$			3		1	4
CrOx		1	1	4	1	7
(Cr,Fe)Ox				3		3
FeOx			7	3	2	12
NaCl/O	1	3	1	4	3	12
$NaNO_3$	3	95	21	28	14	161
Na_2SO_4		5	2	2	10	19
$Na(NO_3,SO_4)$		3	2	2	1	8
$Na(NO_3,Cl)$		6	3	2	1	12
$Na(NO_3,SO_4,Cl)$		2		3		5
$Na(SO_4,Cl)$		6			2	8
(Na,Mg)Cl/O		42	25	5	3	75
$(Na,Mg)NO_3$	1	16	29	58	72	176
$(Na,Mg)SO_4$		1	2	1	5	9
$(Na,Mg)(NO_3,Cl)$			11	14	3	28
$(Na,Mg)(SO_4,Cl)$				1	5	6
$(Na,Mg)(NO_3,SO_4)$		4	3	3	10	20
$(Na,Mg)(NO_3,SO_4,Cl)$			5	1	5	11
$(NH_4)_2SO_4$	1		3	9	60	73
SiO_2	8	2	3	13	11	37
SiO_2/carb			6			6
C/S/O			2		4	6
Cl/O				4		4
Cl/C		5	5			10
Cl/C/Na/O		14	2			16
Na/Mg/O			1	4	3	8
others[d]	2	9	14	10	9	44
NEIC[e]	3	7	29	33	32	104
sum	88	300	300	300	300	1288

[a] The aerodynamic cutoff diameters for stages 1−5 are 16, 8, 4, 2, and 1 μm, respectively. [b] AlSi, aluminosilicates. [c] Carb, carbonaceous species. [d] Others, particle type with less than 1% frequency in all the stages (19 types: $Ca(CO_3,SO_4)$, CuOx, CuOx/carb, KNO_3, $K(CO_3,NO_3)$, $(Na,Ca)CO_3$, Na_2SO_4/carb, $(Na,Ca)SO_4$, $(Na,Mg,Ca)NO_3$, $(NH_4,Na)SO_4$, $(NH_4,Ca)SO_4$, NiOx, $MgCO_3$, $MgCl_2$, $MgCl_2$/N/S, SiO_2/Fe, TiOx, Cl/Mg/O, Cl/S/O). [e] NEIC, X-ray spectra for the particles do not have enough information for classification.

Overall, 2888 particles for two samples were analyzed, and the results of classification based on chemical species of the particles are shown in Table 1 for the Kosan sample and in Table 2 for the 1100 Hill sample. All together, 52 and 48 different particle types were identified for the Kosan and the 1100 Hill samples, respectively. Soil-derived particles such as aluminosilicates, $CaCO_3$, SiO_2, and iron oxides; carbonaceous particles; and particles originated from marine aerosols are very frequently observed in those two samples. Particles containing carbonaceous species, either as single species or mixed with others, are the most frequently observed (890 out of total measured 2888 particles: 30.8%), followed by particles containing $NaNO_3$ (637/2888: 22.1%), aluminosilicates (278/2888: 9.6%), $(NH_4)_2SO_4$ (240/2888: 8.3%), Na_2SO_4 (134/2888: 4.6%), SiO_2 (102/2888: 3.5%), and NaCl

TABLE 2. Particle Types and Numbers of Particles Found in 1100 Hill Sample[a]

	no. of particles						
particle type	stage 1	stage 2	stage 3	stage 4	stage 5	stage 6	sum
Al_2O_3	1	12	8	13	22	5	61
AlSi[b]	4	33	7	7	19	7	77
AlSi/carb[c]	9	44	27	27	13	3	123
biogenic	59	72	81	70	13	7	302
carbon-rich	3	5	5	4	13	3	33
organic	12	13	16	17	3	6	67
$CaCO_3$	1	4	15	6		1	27
$CaCO_3$/carb	2	7	10	1			20
$CaSO_4$/carb		5	5		2		12
CrOx			3	1			4
FeOx	1	1	2	6	12	3	25
FeOx/carb	1	7	3	6			17
KNO_3/carb		1	1	3			5
$NaNO_3$		3		4	1		8
Na_2SO_4			3	2	3	1	9
$(Na,Mg)NO_3$		49	54	46	13		162
$(Na,Mg)SO_4$			1	1	7		9
$(Na,Mg)(NO_3,Cl)$		7	3				10
$(Na.Mg)(NO_3,SO_4)$		4	5	13	8		30
$(NH_4)_2SO_4$				11	79	63	153
$(NH_4)_2SO_4$/carb			2	3		2	7
$(NH_4)_2SO_4$/AlSi				2	5		7
SiO_2	1	7	4	15	15	3	45
SiO_2/carb	3	6	4	1			14
S/O			4	5	38	75	122
others[d]	2	5	16	18	12	2	55
NEIC[e]	1	15	21	18	22	119	196
sum	100	300	300	300	300	300	1600

[a] The aerodynamic cutoff diameters for stages 1−6 are 16, 8, 4, 2, 1, and 0.5 μm, respectively. [b] AlSi, aluminosilicates. [c] Carb, carbonaceous species. [d] Others, particle type with less than 1% frequency in all the stages (23 types: Al_2O_3/carb, $Ca(CO_3,NO_3)$, $(Ca,K)CO_3$, $(Ca,Mg)CO_3$, $(Ca,Mg)SO_4$, (Co,Fe,Ni)Ox, (Cr,Fe)Ox, (Cr,Fe,Ni)Ox, CuOx, K_2CO_3, K_2SO_4, KNO_3, $(K,NH_4)SO_4$, $MgCO_3$, $NaNO_3$/AlSi, Na_2SO_4/AlSi, $(Na,Ca)SO_4$, $(Na,K)SO_4$, $(Na,NH_4)SO_4$, $(Na,NH_4,K)SO_4$, (Na,Mg)Cl/O, $NH_4(SO_4,NO_3)$, TiOx/AlSi). [e] NEIC, X-ray spectra for the particles do not have enough information for classification.

(89/2888: 3.1%). Since the sampling sites are considered to be minimally influenced by local anthropogenic emissions, the abundant observations of some particle types, e.g., biogenic (one type of carbonaceous species) and soil-derived particles, imply strong influence from local natural sources.

Even though the two sampling sites are not located far from each other and the air mass delay between two sampling times is ca. 5 h, there exist some differences in the characteristics of aerosol particles between the two, mainly because of their different surroundings; one is close to the coast, and the other is in the forest. Aerosol particles originated from sea salts are relatively more frequently encountered at Kosan, whereas soil-derived, carbonaceous, and anthropogenic particles predominate at 1100 Hill. As shown in Figure 2, particles containing NaCl, $NaNO_3$, and Na_2SO_4 species are relatively more abundant in the Kosan sample. In contrast, particles containing carbonaceous species (most of them are biogenic particles) and also soil-derived particles, e.g., containing aluminosilicates and iron oxides, and $(NH_4)_2SO_4$-containing particles are relatively more abundant in the 1100 Hill sample. A more detailed discussion on the characteristics of the aerosol particles is given later.

Since EPMA can provide information on the morphology of individual particles as well as on chemical composition, the size distributions of particles at different stages of the May cascade impactor were investigated. The EPMA measurements were done in automatic data acquisition mode, where the electron beam is aligned at the center of particles by a computer using a homemade software before acquiring data from each particle while scanning over the particle. The size of particles is automatically saved in the computer after being converted to that of equivalent spherical particles. Figure 3 shows the number distributions of particles in each stage, based on their size, for the Kosan sample. The aerodynamic cutoff diameters for stages 1−5 are specified as 16, 8, 4, 2, and 1 μm, respectively, at a 20 L/min sampling flow. The number distribution according to their real projected physical size of individual particles at each stage is much more complex than believed; some stages have multiple maxima in their number distributions and the two samples show somewhat different number distributions even though the very same impactor was used for aerosol particle collections. A summary for the number distributions of the two samples is given in Table 3. Overall, as the stage number increases and the aerodynamic cutoff size decreases, the peak maxima of the number distributions also decrease. Since we are dealing with real projected physical sizes measured by EPMA, multiple peak maxima are observed mainly because particle groups with different densities are collected in the stages (shattering of particles at their impaction could be a reason for the maxima found at a smaller size than the apparent cutoffs of the impactor). The stages of the May impactor are supposed to separate aerosol particles based on their aerodynamic diameter, which is defined as the equivalent diameter of spherical particles with density of 1.0. For example, the observation of three maxima in the number distribution implies that the stage collected particle groups with three different average densities. For stages 1 and 2 of the Kosan sample, the real physical sizes are smaller than their aerodynamic cutoffs, implying that particles have a somewhat larger density than 1.0. In contrast, the number distributions of stages 1 and 2 for the 1100 Hill sample show the first maximum at sizes larger than or similar to their aerodynamic cutoffs, implying that some particles collected at these stages have a lower density. In the same context, it could be claimed that stages 4−6 collected some lighter (the first maximum in number distributions) and also heavier (the second and third maxima) particles. This result shows the complex nature of the size segregation during the sampling using a cascade impactor, and it is somewhat difficult to extract useful chemical information only from the number distribution data.

TABLE 3. Summary of Number Distributions for Kosan and 1100 Hill Samples

		Kosan			1100 Hill		
stage	aerodynamic cutoff diameter[a]	1st max	2nd max	3rd max	1st max	2nd max	3rd max
1	16	15.8	10.0	5.0	20.0	7.9	
2	8	6.3	4.0	2.3	7.9	2.5	
3	4	4.0	2.3	1.3	6.3	2.5	1.3
4	2	4.0	1.3	0.8	4.0	1.6	1.0
5	1	1.6	0.4		1.3	0.4	
6	0.5				0.8		

[a] In μm.

Characteristics of Aerosol Particles Collected at Kosan and 1100 Hill. Despite the relatively short distance (ca. 30 km) between the two sampling sites, Kosan and 1100 Hill, we observed significant differences in the aerosol characteristics between the two samples. Figure 4 shows 3-day back-trajectories of the air mass for our samplings. It was in the Northeast Provinces of China, passed over the Yellow Sea and the Korea peninsula, and had stagnated over the strait between Korea and Japan for 1 day before arriving at Cheju Island. From the back-trajectory data, it can be said that the air mass had mostly been under marine influence and maybe some from Korea and Japan before arriving at the sampling sites.

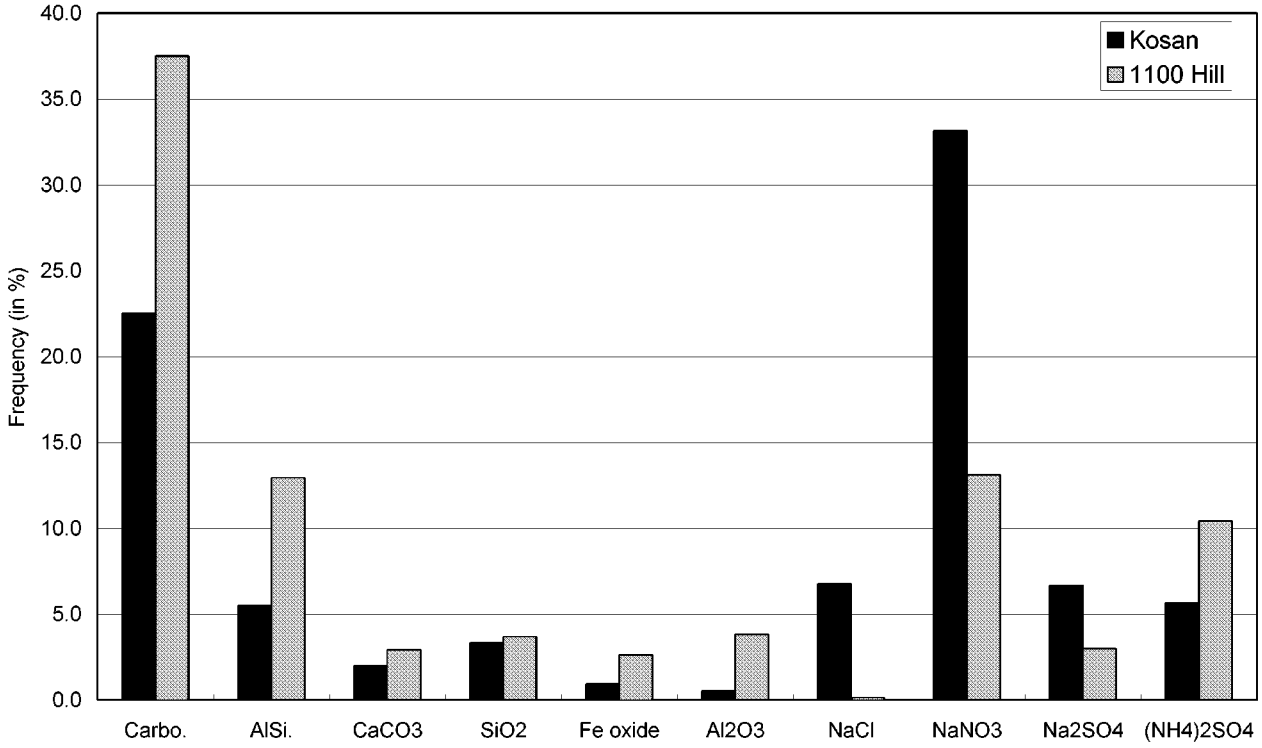

FIGURE 2. Frequencies of 10 major groups of particles containing specified chemical species in Kosan and 1100 Hill samples (carb, carbonaceous species; AlSi, aluminosilicates).

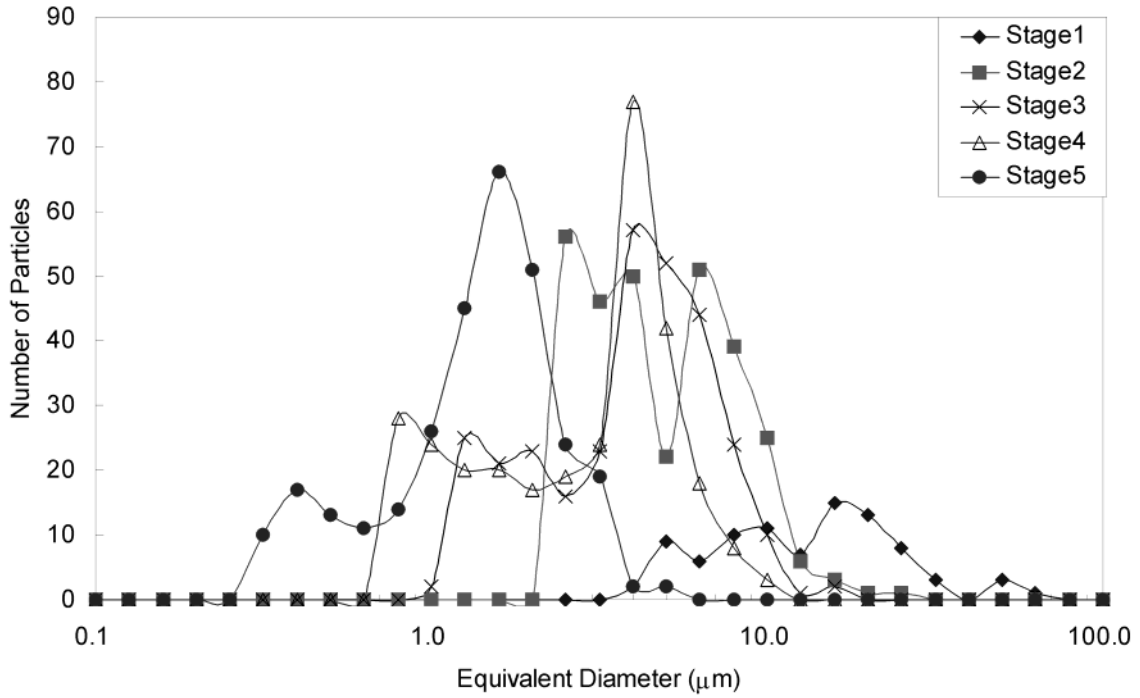

FIGURE 3. Number distributions of particles at each stage, based on their size, in the Kosan sample.

Marine-Originated Particles. As shown in Tables 1 and 2 and Figure 2, one of the most abundant particle types is marine-originated, and there are some strong implications that sea salts had reacted with other chemical species before the samplings. For example, the chance to observe "genuine" sea-salt particles (e.g., NaCl/O and (Na, Mg)Cl/O particle types given in Tables 1 and 2) is relatively very small (89/2888: 3.1%) as compared to "reacted sea-salt" particles (e.g., $NaNO_3$- and Na_2SO_4-containing ones (871/2888: 30.2%)). Only Na, Cl, and O are observed for genuine NaCl particles, which contain some moisture (the EPMA technique cannot detect H). In contrast, we observed a number of reacted sea-salt particles; e.g., $NaNO_3$ particles that are observed frequently in the Kosan sample (161/1288: 12.5%). Also internally mixed particles with $NaNO_3$ and $Mg(NO_3)_2$ are abundant; 13.7% for the Kosan sample and 10.1% for the 1100 Hill sample. In addition, particles containing Na_2SO_4 and/or $MgSO_4$ species are also observed (134/2888: 4.6%). We also observed a significant number of Na- and Mg-containing particles with Cl as well as other chemical species,

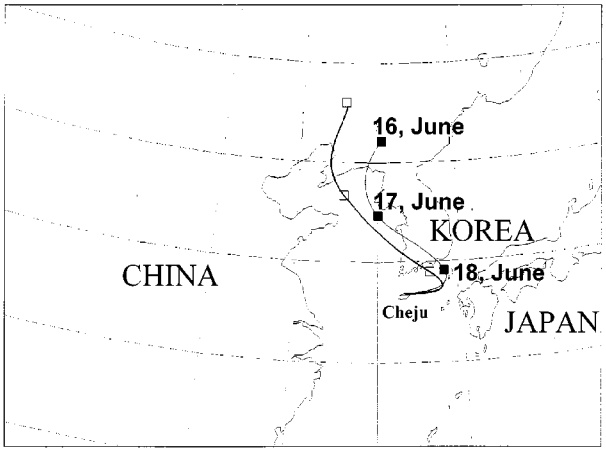

FIGURE 4. Air mass back-trajectory for Kosan (thin line) and 1100 Hill (thick line) samples.

e.g., (Na,Mg)(NO_3,Cl), (Na,Mg)(SO_4,Cl) and (Na,Mg)(NO_3,-SO_4,Cl) types, implying that the reactions between sea salts and the other species were not complete so that the particles still have some remnant Cl in them. Finally, we calculated the ratio of atomic concentrations between Na and Mg in all the mixture particles containing $NaNO_3$ and $Mg(NO_3)_2$, i.e., 338 particles. The ratio is 0.128 with a relative standard deviation of 4.7%, which is remarkably similar to that of seawater: 0.122 (*32*). This result provides strong evidence for the original source of those particles; they were from the sea and reacted with HNO_3 in air.

Some works based on size-segregated bulk analysis claimed that nitrate and sulfate particles are formed from sea salts. Zhuang et al. (*33*) reported that significant chloride depletion (74−88%) from coarse-mode sea-salt aerosols was observed and that nitrate accounted for 65% of chloride depletion when their sampling site (Hong Kong) was under prevailing easterly wind accompanied by high relative humidity. For aerosols collected at a site near the Arctic Ocean, the main components replacing chloride from supermicrometer sea-salt particles were reported to be sulfate and nitrate followed by methanesulfonate and oxalate (*34*). In addition to the bulk analysis works, some single-particle analysis also reported nitrate formation from sea salts; e.g., reaction between sea salts and HNO_3 to produce $NaNO_3$ was observed to occur in the atmosphere in a relatively short time by the application of the ATOFMS technique (*15*). Also, our analyses on the aerosols collected over the North Sea strongly support that the reaction occurs in the air when the continental influence dominates on the aerosols over the North Sea (*3*). However, our results presented here based on quantitative analysis on Na and Mg concentration in nitrate particles might be the most direct proof of nitrate formation from sea salt up to now.

One other result by Chen et al. (*19*) is that Cl is significantly depleted in sea-salt aerosols at Kosan, implying that many sea salts react. However, it was suggested that nitrate is most strongly correlated with non-sea-salt (nss) Ca, and thus nitrate at Cheju Island seemed mostly to be calcium nitrate. In their work, anions and cations in the aerosols were analyzed using bulk analysis, and it was found that the nss Ca concentrations were positively related to those of nitrate by application of principal component analysis, especially when Kosan was strongly dominated by continental influence. Their result is obtained from data collected over 3 yr (March 1992−February 1995), and thus, overall, nitrate might exist more as the calcium nitrate species. Our result suggests, however, that $NaNO_3$ should be regarded as one of the important nitrate species in Cheju Island aerosols.

Overall frequencies to observe nitrate particles with Na and/or Mg species are higher in the Kosan sample than in the 1100 Hill sample (33.2% vs 13.1%). Also, genuine sea salts are not observed in the 1100 Hill sample, whereas those are quite frequently encountered in the Kosan sample (6.9%). The 1100 Hill sample was less loaded by marine-originated particles since the 1100 Hill site is some 30 km inland from Kosan. There was also a 5-h time difference between collections of the two samples, where the 1100 Hill sample was collected later. When considering the back-trajectory data, the locations of the two sampling sites, and the sampling times, it is expected that aerosol particles of marine origin collected at 1100 Hill are somewhat more aged than those at Kosan.

In the Kosan sample, particles composed only of $NaNO_3$ species are frequently observed as much as particles with mixed $NaNO_3$ and $Mg(NO_3)_2$ species, and yet in the 1100 Hill sample, those of only $NaNO_3$ species are much less frequent than those of $NaNO_3$ and $Mg(NO_3)_2$ species. Also, NaCl particles are observed at Kosan, although less frequently than NaCl and $MgCl_2$ mixture particles. There is a good possibility that those nitrate and chloride particles which contain only Na, also contain Mg at trace levels, because the detection limits of ED-EPMA are in the range of 0.1−1 wt %. However, the average atomic concentrations of Na and Mg elements in all the particles containing both $NaNO_3$ and $Mg(NO_3)_2$ species are 14.8% and 1.9%, respectively. In contrast, those of Na and Mg elements in all the $NaNO_3$ particles are 19.8% and 0.3%, respectively. No particle identified as $NaNO_3$ and NaCl species contains a Mg content larger than 1% in atomic fraction. In other words, two types of sea salts were indeed observed in the Kosan sample, with and without Mg.

The Na-containing and the Na- and Mg-containing nitrate particles were collected in the different proportions at the different stages. At the stage with larger cutoff diameter, e.g., stage 2, the $NaNO_3$ particles are relatively more frequently encountered than the Na- and Mg-containing nitrate particles. The situation is reversed for the stages of relatively smaller cutoffs, e.g., stages 4 and 5, where the $NaNO_3$ particles are relatively less frequently encountered. It implies that the $NaNO_3$ particles were denser, namely, of more crystalline nature, than the Na- and Mg-containing nitrate particles, possibly collected in the form of water droplets so that they were collected more at the stages of larger cutoff diameters. The density of $NaNO_3$ is 2.26, whereas that of water droplets is almost 1.0. We also calculated the average sizes of both the $NaNO_3$ particles and the Na- and Mg-containing nitrate particles at each stage. The result strongly supports our argument that the $NaNO_3$ particles were collected as crystalline form whereas the Na- and Mg-containing nitrate particles were collected more as water drops; the sizes of the $NaNO_3$ particles are much smaller than those of the Na- and Mg-containing nitrates (e.g., 3.53 vs 7.14 μm for stage 2, 2.95 vs 4.64 μm for stage 3, 1.86 vs 3.70 μm for stage 4, and 1.35 vs 1.55 μm for stage 5).

We do not believe that the $NaNO_3$ particles were fractionally recrystallized on the stages after collecting aerosol particles because the particles were confirmed to be well-separated from the other particles using scanning electron microscopy. There was also a report claiming that some of the aerosol particles sampled over the Southern Ocean using an impactor were collected with fractional recrystallization within evaporating seawater drops followed by shattering (*35*). During our sampling, the relative humidity was around 75%, which is very close to deliquescence points of NaCl (75%) and $NaNO_3$ (74%) (*36*), and thus some of NaCl- and $NaNO_3$-containing particles might be crystalline in the air before the sampling. It was reported that muticomponent aerosols showed smooth transitions in the hysteresis paths of particle size with relative humidity instead of the sharp

steps of a pure salt (*37*). In addition, deliquescence point or water activity of a multicomponent system is lower when compared to that of each single-component solution as shown for an NH_4NO_3/NH_4Cl system (*38*). This kind of lowering of deliquescence points for multicomponent systems are well-demonstrated both numerically by using thermodynamic models (*36*) and experimentally (*39*), which possibly explains why $NaNO_3$ particles are in crystalline form whereas Na- and Mg-containing particles (a multicomponent system) are in droplets.

The particles with both $NaNO_3$ and $Mg(NO_3)_2$ species must be formed by the reaction between sea salts and HNO_3 dissolved in seawater droplets because the ratio of Mg content to Na of the particles is the same as that of seawater. Nitrates from sea salts can be formed in the reactions between sea salts and several gaseous nitrogen species such as HNO_3, N_2O_5, NO_2, and $ClONO_2$. Among the nitrogen species, HNO_3 is reported to be the most important in the nitrate formation from sea salts in the marine atmosphere (*40*). In addition, the Henry constant of HNO_3 is higher than the other nitrogen species, and evaporation of nitrate from fine particles to HNO_3 in the gas phase and its subsequent transport to coarse sea-salt particles are well-established both experimentally (*33*) and numerically (*24*). Ten Brink performed kinetic studies on the reactive uptake of HNO_3 and H_2SO_4 in sea-salt particles in a smog chamber, and he found that a measurable reaction between airborne NaCl and HNO_3 only occurred when NaCl particles were present in the form of droplets (*41*). However, it is not clear whether the $NaNO_3$ particles were formed by the reaction of already crystalline NaCl particles and gaseous nitrogen species in the air or whether the $NaNO_3$ particles were recrystallized within evaporating seawater droplets after the reaction.

If, for the $NaNO_3$ particles, the gaseous nitrogen species would react on the surface of the crystalline NaCl particles and if the reaction would not be completely finished, then heterogeneous particles would be formed, e.g., $NaNO_3$ at the surface and NaCl in the core. For the other case, homogeneous particles would be generated. We are currently developing a new EPMA-based method that allows the investigation of the heterogeneity of single particles, and we hope that our further research using the new method can directly and conclusively address this question. The new methodology is based on the use of electron beams with different primary energies. With a 10-kV electron energy, which is the condition used in this study, a 2−3 μm range of single particles depending on the chemical composition is analyzed. When a lower energy of electron (e.g., 5 kV) is used, then a more shallow region of the particles is investigated, whereas the deeper region of the particles is probed with the higher electron energy, such as 15 and 20 kV. If a particle is homogeneous, then the obtained concentrations of chemical elements in the particles will be consistent for the different electron energies. However, if the particle is heterogeneous (for example, NaCl in the core and $NaNO_3$ in the surface), the obtained concentrations of chemical elements from surface species such as N and O will be larger in the data measured by low electron energy than by the higher electron energies, whereas the concentration of Cl will be smaller for the lower electron energy. This approach indeed provides detailed information on the heterogeneity for artificially generated heterogeneous $CaCO_3$−$CaSO_4$ individual particles (*42*).

It is known that heterogeneous sulfur conversion in sea-salt particles might be important (*43*). Also it is reported that the SO_4^{2-} concentration in Cheju island is much higher than NO_3^- on average (*18*, *21*). And thus it can be expected that, at Kosan, Na_2SO_4-containing particles would be observed. However, Na_2SO_4-containing particles are relatively less frequently observed as compared to $NaNO_3$-containing particles (4.6% vs 22.1%). Since it rained a whole day before the sampling, more water-soluble gaseous sulfur species would be washed out more than gaseous nitrogen species.

Carbonaceous Particles. Carbonaceous particles are also abundantly present in both samples. In our previous study, it has been shown that the low-*Z* EPMA can distinguish three different carbonaceous particles, e.g., carbon-rich, organic, and biogenic particles (*31*). Biogenic particles are identified when the C and O contents in the particles are similar, and they also contain some N, P, S, K, and/or Cl contents, which are characteristic elements for biogenic particles. Carbon-rich particles were identified when the sum of the C and O contents is larger than 90% in atomic fraction and the C content is 3 times larger than the O content. Organic particles are identified if the sum of the C and O contents is larger than 90% in atomic fraction, and yet they are not assigned to be either biogenic or carbon-rich particles. Therefore, the carbon-rich particles are somewhat related to elemental carbon (EC) particles, whereas the biogenic particles can be regarded as one type of organic carbon (OC) particles.

As shown in Tables 1 and 2, the major carbonaceous species in the two samples is biogenic (77.4% for the Kosan sample and 75.1% for the 1100 Hill sample). It was reported by Kim et al. (*44*) that, at Kosan, the ratio values of OC and EC concentration levels in $PM_{2.5}$ showed good consistency, except in the summer, when the ratio is higher than for the other seasons. And in their work, it was suggested, based on the concentrations of gaseous volatile organic compounds, that biogenic emissions of OC might be significant during summer, which is confirmed from our results.

The mean concentrations of OC and EC during August 1994 and July 1995 at Kosan for $PM_{2.5}$ were reported as 2.36 and 0.09 $\mu g/m^3$, respectively; the OC content is some 26 times larger than EC in mass base (*20*). In our study, the ratios between the sum of organic and biogenic particles and the number of carbon-rich particles for the particles in stages 4−6 are 17 for the Kosan sample and 6 for the 1100 Hill sample. It is somewhat difficult to correlate the results of this work about carbonaceous particles with bulk analysis data, mainly because our study is on number distributions and the bulk analysis provides concentrations in mass. However, it is clear from our study that the major source of OC is biogenic both at Kosan and at 1100 Hill.

Soil-Derived Particles. Soil derived particles, such as aluminosilicates, iron oxide, and $CaCO_3$, are quite frequently encountered. Since the air mass had been mostly under marine influence, most of these soil-derived particles are probably from local sources. Two types of aluminosilicate-containing particles are identified; aluminosilicate particles (represented as "AlSi" in Tables 1 and 2) and particles mixed with aluminosilicate and carbonaceous species (represented as AlSi/carb). There are many different types of aluminosilicate minerals, and yet we just classified the particles as aluminosilicate when silicon and aluminum oxides are the major components. The aluminosilicate-containing particles constitute 5.5% (71 particles/total 1288) of the Kosan sample and 12.5% (200/1600) of the 1100 Hill sample. They are significantly observed in all stages for both samples. These particles are much more abundant in the 1100 Hill sample. Also, mixed particles of aluminosilicate and carbonaceous species are abundant in the 1100 Hill sample (123/1600; 7.7%), suggesting two possibilities. One is that the mixed particles are just from the local area, so that the particles contain carbonaceous species from humic materials in soil. Another possibility is the existence of reactions between aluminosilicate and carbonaceous particles. Since the mixture particles are observed more in the 1100 Hill sample, where the carbonaceous, especially biogenic, particles are greatly abundant, the latter possibility may not be excluded.

Iron oxide-containing particles are believed to originate from local soils. They are observed more abundantly in the 1100 Hill sample (42/1600; 2.6%) than in the Kosan sample (12 /1288; 0.9%). For the 1100 Hill sample, iron oxide particles mixed with carbonaceous components are encountered almost as frequently as iron oxide particles as single species (17 vs 25). Soil-derived $CaCO_3$-containing particles are also frequently encountered; 2.0% at Kosan and 2.9% at 1100 Hill. SiO_2-containing particles are observed in similar parts both at Kosan (43/1288; 3.3%) and at 1100 Hill (59/1600; 3.7%). In addition, chromium-containing particles in both samples are observed, although in low abundance. Some of them are mixed with iron and/or nickel oxides. Al_2O_3 particles are observed in a significant amount, especially for the 1100 Hill sample (61 particles out of total 1600; 3.8%). It is not clear whether these are from local soil. However, since the number of these particles is just 7 out of the total of 1288 (0.5%) for the Kosan sample and these particles are mostly observed at stage 1 (its cutoff diameter is 16 μm), this is probably the case. Also, these particles are encountered frequently at all the stages, which is the same for aluminosilate-containing (soil-derived) particles. However, further investigation on the local soils would help to conclusively determine the source of this type of particles.

$(NH_4)_2SO_4$ Particles. Among particles with other chemical species, $(NH_4)_2SO_4$ particles are significantly observed in both the Kosan and the 1100 Hill samples; they are regarded to have anthropogenic origins. The particles are more frequently encountered at the stages of smaller cutoff diameters, reflecting that they are small in size and formed from gaseous species. For the 1100 Hill sample, they sometimes also contain carbonaceous or aluminosilicate species.

Acknowledgments

This work was supported by a Korea Research Foundation Grant (KRF-2000-015-DP0453) and partially by the Flemish Foundation for Scientific Research (FWO-Vlaanderen).

Literature Cited

(1) Jambers, W.; De Bock, L.; Van Grieken, R. *Analyst* **1995**, *120*, 681−692.
(2) Ro, C.-U.; Osan, J.; Van Grieken, R. *Anal. Chem.* **1999**, *71*, 1521−1528.
(3) Osan, J.; Szaloki, I.; Ro, C.-U.; Van Grieken, R. *Mikrochim. Acta* **2000**, *132*, 349−355.
(4) Szaloki, I.; Osan, J.; Ro, C.-U.; Van Grieken, R. *Spectrochim. Acta* **2000**, *B55*, 1017−1030.
(5) Weinbruch, S.; Wentzel, M.; Kluckner, M.; Hoffman, P.; Ortner, H. M. *Mikrochim. Acta* **1997**, *125*, 137−141.
(6) Roth, B.; Okada, K. *Atmos. Environ.* **1998**, *32*, 1555−1569.
(7) Mamane, Y.; Gottlieb, J. *Atmos. Environ.* **1992**, *26A*, 1763−1769.
(8) Mamane, Y.; Gottlieb, J. *J. Aerosol Sci.* **1989**, *20*, 575−584.
(9) Mamane, Y.; Gottlieb, J. *J. Aerosol Sci.* **1989**, *20*, 303−311.
(10) Carson, P. G.; Johnston, M. V.; Wexler, A. S. *Aerosol Sci. Technol.* **1997**, *26*, 291−300.
(11) Noble, C. A.; Prather, K. A. *Environ. Sci. Technol.* **1996**, *30*, 2667−2680.
(12) Gard, E.; Mayer, J. E.; Morrical, B. D.; Dienes, T.; Fergenson, D. P.; Prather, K. A. *Anal. Chem.* **1997**, *69*, 4083−4091.
(13) Murphy, D. M.; Thomson, D. S. *J. Geophys. Res.* **1997**, 102, 6341−6352.
(14) Murphy, D. M.; Thomson, D. S. *J. Geophys. Res.* **1997**, 102, 6353−6368.
(15) Gard, E. E.; Kleeman, M. J.; Gross, D. S.; Hughes, L. S.; Allen, J. O.; Morrical, B. D.; Fergenson, D. P.; Dienes, T.; Galli, M. E.; Johnson, R. J.; Cass, G. R.; Prather, K. A. *Science* **1998**, *279*, 1184−1187.
(16) Kim, Y. P.; Lee, J. H.; Baik, N. J.; Kim, J. Y.; Shim, S.-G.; Kang, C.-H. *Atmos. Environ.* **1998**, *32*, 3905−3915.
(17) Carmichael, G. R.; Zhang, Y.; Chen, L.-L.; Hong, M.-S.; Ueda, H. *Atmos. Environ.* **1996**, *30*, 2407−2416.
(18) Carmichael, G. R.; Hong, M.-S.; Ueda, H.; Chen, L.-L.; Murano, K.; Park, J. K.; Lee, H.; Kim, Y.; Kang, C.; Shim, S. *J. Geophys. Res.* **1997**, *102*, 6047−6061.
(19) Chen, L.-L.; Carmichael, G. R.; Hong, M.-S.; Ueda, H.; Shim, S.; Song, C. H.; Kim, Y. P.; Arimoto, R.; Prospero, J.; Savoie, D.; Murano, K.; Park, J. K.; Lee, H.; Kang, C. *J. Geophys. Res.* **1997**, *102*, 28551−28574.
(20) Kim, Y. P.; Moon, K.-C.; Lee, J. H. *Atmos. Environ.* **2000**, *34*, 3309−3317.
(21) Lee, H. H.; Kim, Y. P.; Moon, K.-C.; Kim, H.-K.; Lee, C. B. *Atmos. Environ.* **2001**, *35*, 635−643.
(22) Hayami, H.; Carmichael, G. R. *Atmos. Environ.* **1998**, *32*, 1427−1434.
(23) Hayami, H.; Carmichael, G. R. *Atmos. Environ.* **1997**, *31*, 3429−3439.
(24) Song, C. H.; Carmichael, G. R. *Atmos. Environ.* **1999**, *33*, 2203−2218.
(25) Strees, D. G.; Tsai, N. Y.; Akimoto, H.; Oka, K. *Atmos. Environ.* **2000**, *34*, 4413−4424.
(26) May, K. R. *J. Aerosol Sci.* **1975**, *6*, 1−7.
(27) Vekemans, B.; Janssens, K.; Vincze, L.; Adams, F.; Van Espen, P. *X-Ray Spectrom.* **1994**, *23*, 278−285.
(28) Drouin, D.; Hovington, P.; Gauvin, R. *Scanning* **1997**, *19*, 20−28.
(29) Hovington, P.; Drouin, D.; Gauvin, R. *Scanning* **1997**, *19*, 1−14.
(30) Ro, C.-U.; Oh, K.-Y.; Kim, H.; Chun, Y.-S.; Osan, J.; de Hoog, J.; Van Grieken, R. *Atmos. Environ.* **2001**, *35*, 4995−5005.
(31) Ro, C.-U.; Osan, J.; Szaloki, I.; Oh, K.-Y.; Kim, H.; Van Grieken, R. *Environ. Sci. Technol.* **2000**, *34*, 3023−3030.
(32) Weast, R. C., Astle, M. J., Beyer, W. H., Eds. *CRC Handbook of Chemistry and Physics*; CRC Press: Boca Raton, FL, 1984; p F-154.
(33) Zhuang, H.; Chan, C. K.; Fang, M.; Wexler, A. S. *Atmos. Environ.* **1999**, *33*, 4223−4233.
(34) Kerminen, V.-M.; Teinila, K.; Hillamo, R.; Pakkanen, T. *J. Aerosol Sci.* **1998**, *29*, 929−942.
(35) Mouri, H.; Nagao, I.; Okada, K.; Koga, S.; Tanaka, H. *Atmos. Res.* **1997**, *43*, 183−195.
(36) Kim, Y. P.; Seinfeld, J. H.; Saxena, P. *Aerosol Sci. Technol.* **1993**, *19*, 157−181.
(37) Hanel, G.; Lehmann, M. *Contrib. Atmos. Phys.* **1981**, *54*, 57−71.
(38) Wexler, A. S.; Seinfeld, J. H. *Atmos. Environ.* **1991**, *25A*, 2371−2748.
(39) Ha, Z.; Choy, L.; Chan, C. K. *J. Geophys. Res.* **2000**, *105*, 11699−11709.
(40) Fenter, F. F.; Caloz, F.; Rossi, M. J. *J. Phys. Chem.* **1996**, *100*, 1008−1019.
(41) Ten Brink H. M. *J. Aerosol Sci.* **1998**, *29*, 57−64.
(42) Ro, C.-U.; Oh, K.-Y.; Osan, J.; de Hoog, J.; Worobiec, A.; Van Grieken, R. *Anal. Chem.* **2001**, *73*, 4574−4583.
(43) Sievering, H.; Boatman, J.; Galloway, J.; Keene, W.; Kim, Y.; Luria, M.; Ray, J. *Atmos. Environ.* **1991**, *25A*, 1479−1487.
(44) Kim, Y. P.; Moon, K.-C.; Shim, S.-G.; Lee, J. H.; Kim, J. Y.; Fung, K.; Carmichael, G. R.; Song, C. H.; Kang, C. H.; Kim, H.-K.; Lee, C. B. *Atmos. Environ.* **2000**, *34*, 5053−5060.

Received for review May 17, 2001. Revised manuscript received September 7, 2001. Accepted September 18, 2001.

ES0155231